HHS Public Access

Author manuscript

Nat Med. Author manuscript; available in PMC 2009 November 03.

Published in final edited form as:

Nat Med. 2009 April ; 15(4): 384–391. doi:10.1038/nm.1939.

HETEROTYPIC INTERACTIONS ENABLED BY POLARIZED NEUTROPHIL MICRODOMAINS MEDIATE THROMBO-INFLAMMATORY INJURY

Andrés Hidalgo[*,‡], **Jungshan Chang**[*], **Jung-Eun Jang**[*], **Anna J. Peired**[*], **Elaine Y. Chiang**[*,∇], and **Paul S. Frenette**[*,¶,#]

[*]Mount Sinai School of Medicine, Departments of Medicine, New York, NY 10029.

[¶]Gene and Cell Medicine, Black Family Stem Cell Institute, New York, NY 10029.

[#]Immunology Institute, New York, NY 10029.

Abstract

Selectins and their ligands mediate leukocyte rolling allowing interactions with chemokines that lead to integrin activation and arrest. Here, we demonstrate that E-selectin is critical to induce a secondary wave of activating signals transduced specifically by E-selectin ligand-1, that induces polarized, activated αMβ2 integrin clusters at the leading edge of crawling neutrophils, allowing the capture of circulating erythrocytes or platelets. In a humanized model of sickle cell disease (SCD), the capture of erythrocytes by αMβ2 microdomains leads to acute lethal vascular occlusions. In a model of transfusion-related acute lung injury, polarized neutrophils capture circulating platelets, resulting in the generation of oxidative species that produces vascular damage and lung injury. Inactivation of E-selectin or αMβ2 prevented tissue injury in both inflammatory models, suggesting broad implications of this paradigm in thrombo-inflammatory diseases. These results indicate that endothelial selectins can influence neutrophil behavior beyond its canonical rolling step through delayed, organ-damaging, polarized activation.

Leukocytes are recruited to inflamed areas by a tightly regulated cascade of adhesive and signaling events that choreograph their migration. Neutrophil (PMN) rolling is mediated by endothelial P- and E-selectins (encoded by *Selp* and *Sele*, respectively)1–3. Three glycoproteins, P-selectin glycoprotein ligand-1 (PSGL-1, encoded by the *Selplg* gene), E-selectin ligand-1 (ESL-1, encoded by *Glg1*), and CD44 (encoded by *Cd44*) mediate the physiological binding of murine PMNs to endothelial selectins through highly specialized

Address correspondence to Paul S. Frenette (paul.frenette@mssm.edu) or Andrés Hidalgo (andres.hidalgo@mssm.edu), Mount Sinai School of Medicine, One Gustave L. Levy Place, Box 1079, New York, NY 10029. Tel: (212) 659-9693; Fax: (212) 849-2574.

[‡]Present address: Department of Atherothrombosis and Cardiovascular Imaging, Centro Nacional de Investigaciones Cardiovasculares, Madrid 28029, Spain.

[∇]Present address: University of Pennsylvania, Penn Comprehensive Hemophilia and Thrombosis Program, Penn Presbyterian Medical Center, Philadelphia, PA 19104.

Author contributions

A.H. conceived the study, performed experiments, analyzed data and wrote the manuscript; J.C. performed experiments and analyzed data; A.J.P. maintained and generated the mice used in this study; J.J. performed experiments and analyzed data; E.Y.C. performed experiments and analyzed data; P.S.F. conceived the study, supervised the overall project, analyzed data and wrote the manuscript.

contributions4. Leukocyte rolling is followed by a first wave of endothelial signals that activate integrins, allowing firm arrest. Although G-protein coupled receptor (GPCR)-induced signaling triggered by chemokines is the best characterized pathway, recent studies have uncovered physiological signaling functions for E-selectin ligands (ESLs). On rolling leukocytes CD44-mediated signaling participates in receptor redistribution4, whereas PSGL-1 induces partial activation of αLβ2 integrin (LFA-1)5. Although *Glg1* sequence is homologous to the fibroblast growth factor receptor gene6, it remains unknown whether ESL-1 can transduce signals. E-selectin engagement can also activate the integrin αMβ2 (CD11b/CD18, Mac-1) on PMNs7,8, but the actual ESL involved in this process has not been identified. αMβ2 binds promiscuously endothelial counter-receptors, matrix and plasma proteins9, the complement fragment C3b10 and GpIbα on platelets11, thus contributing to leukocyte recruitment and platelet adhesion.

During recruitment, leukocytes rapidly polarize, redistributing chemokine receptors12, activated β2 integrins13 and actin-remodeling GTPase clusters14 at the leading edge whereas the trailing edge (uropod) is enriched in heavily glycosylated proteins (e.g. PSGL-1, L-selectin, CD43) and other components involved in membrane retraction12,14. These microdomains are important for the directional, chemokine-driven movement of leukocytes within blood vessels and across the endothelium.

Activated neutrophils recruited to inflamed areas mediate acute and chronic organ injury, as their infusion or increased number in circulation are sufficient to promote organ damage, while their depletion can curb it in multiple experimental or clinical settings15–17. In sickle cell disease (SCD), alterations in the sickle erythrocyte (sRBC) structure cause a pro-inflammatory phenotype that promotes acute vaso-occlusive (VOC) episodes18,19. In a humanized murine model of SCD, PMNs capture circulating sRBC and the rate of these interactions correlates with reductions in microcirculatory blood flow and death20,21. The molecular basis of these interactions, however, has not yet been elucidated. SCD patients and other acutely ill individuals requiring blood transfusions are at risk of transfusion-related acute lung injury (TRALI), the most prevalent cause of transfusion-associated morbidity, where antibodies against the recipient's PMNs or other bioactive mediators from the transfused blood can elicit organ injury22,23.

Here, we demonstrate that the generation of activated integrin microdomains at the leading edge of PMNs emerges from secondary signaling events induced by endothelial E-selectin, and drives vascular damage in TRALI and SCD through heterotypic interactions.

RESULTS

Heterotypic interactions are induced during inflammation

We have examined the cremasteric vasculature of wild-type mice after surgical trauma or following the administration of TNF-α. Brightfield intravital microscopy revealed frequent interactions between adherent leukocytes and red blood cells carrying normal hemoglobin (nRBC) in cytokine-activated venules (Fig.1a–b). These interactions, which tend to occur in venules with relatively low shear rates ($< 500\ s^{-1}$), can last up to several seconds (Supplementary video 1). Endogenous platelets, identified by *in vivo* labeling with an anti-

CD41 antibody24 (Fig.1a and Supplementary video 2), also interacted with adherent leukocytes in venules after surgical manipulation, and these interactions were sharply enhanced after TNF-α treatment (Fig.1c). We mapped the leukocyte microdomains mediating these interactions by high-speed multichannel fluorescence intravital microscopy (MFIM) using clustered L-selectin expression as a marker of the trailing edge25. nRBC interactions were mediated almost exclusively by the leading edge of leukocytes adherent in inflamed venules (Fig.1d and Supplementary video 1). Platelet interactions with leukocytes adherent in non-inflamed venules (surgical trauma alone) were mediated by both the trailing and leading edges (Fig.1e). However, after cytokine-induced inflammation, the marked increase in platelet interactions was mediated by the leading edge (Fig.1e). These results indicate differential contributions of leukocyte microdomains in mediating interactions with blood components under inflammatory conditions.

Heterotypic Interactions are regulated by E-selectin and mediated by αMβ2

Using a humanized model of SCD, we have previously shown that endothelial selectins participate in leukocyte recruitment and VOC21. We thus investigated the individual roles of each endothelial selectin in the capture of nRBCs. The rate of nRBC interactions per adherent leukocyte were significantly reduced in E-selectin-deficient (*Sele*$^{-/-}$), but not P-selectin-deficient (*Selp*$^{-/-}$), mice (Fig.2a). A similar reduction was found in *Sele*$^{-/-}$ mice for platelet captures by adherent leukocytes (Fig.2b), and mainly affected those mediated by the leading edge (Fig.2c). Since E-selectin expression is restricted to the endothelium, these results suggest that signals emanating from the endothelial cells, transmitted by ESLs into leukocytes, regulate these heterotypic interactions.

Since PSGL-1, ESL-1, and CD44 comprise virtually all selectin binding activity on mouse PMNs4 we evaluated the behavior of circulating RBCs in *Selplg*$^{-/-}$ or *Cd44*$^{-/-}$ mice, or lethally irradiated mice reconstituted with hematopoietic cells transduced with a lentiviral vector carrying a short hairpin RNA interference vector against *Glg1* (shESL-1). While no significant reduction in RBC captures was observed in mice lacking either PSGL-1 or CD44 (Fig.2d), we found a marked reduction in nRBC interactions with shESL-1-transduced leukocytes compared to untransduced leukocytes in the same venules or control chimeras reconstituted with a control scrambled control (Fig.2e). These results suggest that ESL-1 is the E-selectin ligand that mediates the activating signals allowing heterotypic interactions during inflammation. Further, inhibition of Src kinases, but not p38 MAPK or the spleen tyrosine kinase (Syk), led to a reduction in nRBC-leukocyte interactions (Fig.2f) comparable to that found in *Sele*$^{-/-}$ mice or shESL-1 mice, suggesting a role for Src kinases in transducing these activating signals.

Activated β2 integrins have been reported to localize at the leading edge of adherent leukocytes13, and their activity can be modulated by E-selectin and Src kinases5,7,8,26,27. We thus hypothesized that αMβ2 might be the receptor mediating heterotypic interactions. High-speed MFIM analyses revealed that αMβ2 was homogeneously expressed on the surface of adherent leukocytes, including areas interacting with RBCs (Fig.3a). We observed a dramatic reduction in the number of nRBC interacting with leukocytes deficient in αM (encoded by the *Itgam* gene; Fig.3b) despite similar RBC counts among all groups

(Supplementary Table 1). In agreement with this finding, *Selplg*$^{-/-}$ leukocytes, which exhibit increased nRBC interactions (Fig.2d), expressed higher levels of αMβ2 (Supplementary Fig.1). Interestingly, mice deficient in the C3 complement protein, a ligand for αMβ2[10], exhibited a significant, but partial, reduction in the frequency of nRBC interactions (Supplementary Fig.2), suggesting that complement opsonization of nRBCs is involved in RBC capture. A dramatic reduction in platelet interactions was also observed with *Itgam*$^{-/-}$ leukocytes (Fig.3c). This reduction was not as marked as that of nRBCs, likely due to integrin-independent interactions at the trailing edge (Fig.3d). These data indicate that the integrin αMβ2 is the receptor mediating heterotypic interactions at the leading edge of adherent leukocytes and that its activity is increased during inflammation.

ESL-1 regulates αMβ2 activity on neutrophil microdomains

The aforementioned observations suggest that E-selectin / ESL-1 controls the activation of αMβ2 on adherent leukocytes. To investigate further this hypothesis, we have developed a novel *in vivo* assay to determine αMβ2 activity on adherent leukocytes in real time. We took advantage of a previously demonstrated property of denatured albumin to bind to leukocytes in a β2 integrin-dependent manner28. We coated fluorescent beads (fluospheres; 1 μm in diameter) with albumin and tracked their behavior by high-speed MFIM after intravenous injection into mice treated with TNF-α (Supplementary video 3). Albumin-coated fluospheres bound exclusively Gr-1^{+} leukocytes, of which the vast majority were PMNs (Gr-1^{+} F4/80^{-}; Fig.4a). Binding was specific since fluospheres coated with polyvinyl alcohol were not captured by leukocytes (Supplementary Fig.3). Fluosphere binding was mediated by the leading edge of adherent PMNs (Fig.4b and Supplementary video 3) and was virtually absent in *Itgam*$^{-/-}$ mice (Fig.4c). In addition, αMβ2 protein expression *in vivo* strongly correlated with avidity (fluosphere capture) (Supplementary Fig.4).

We next used the fluosphere binding assay to determine whether E-selectin engagement could modulate αMβ2 activity *in vivo*. Fluosphere binding in *Sele*$^{-/-}$ venules was significantly reduced compared to wild-type controls or *Selp*$^{-/-}$ venules (Fig.4d). Further, while fluosphere binding was not reduced in mice lacking PSGL-1 or CD44 (Fig.4e) a marked reduction was found in leukocytes transduced with the shESL-1 vector (Fig.4f). These results indicate that ESL-1 regulates regional αMβ2 avidity on the surface of adherent PMNs *in vivo*.

Platelet-neutrophil interactions induce organ injury in TRALI

We next asked whether the induction of heterotypic interactions through this mechanism might underlie the vascular injury that characterizes acute inflammatory processes. Intravenous injection of an anti-MHC-I antibody (haplotype H2d) into Balb/c mice has been used to model TRALI, a process that requires the presence of PMNs17. We induced lung injury in Balb/c mice by intravenous injection of an anti-H2d antibody as assessed by protein accumulation in the alveolar spaces (Fig.5a). A moderate thrombocytopenia developed in these mice (Fig.5b), suggesting that platelets might be involved in the pulmonary pathogenesis in this model. Platelet depletion prior to anti-H2d administration indeed resulted in complete abrogation of protein leakage into the bronchoalveolar space (Fig.5a–b), without affecting PMN recruitment to the lungs (not shown). To investigate the

intravascular events involved in vascular injury, we used high-speed MFIM to observe heterotypic interactions in the cremasteric circulation in mice pre-treated with TNF-α before and after anti-H2d administration. Anti-H2d treatment significantly increased the number of platelet interactions with the leading edge of adherent leukocytes (Fig. 5c–d; Supplementary videos 4a–b), which were inhibited by blocking E-selectin (Fig. 5c). Further, anti-H2d markedly increased the permeability of cremasteric venules, as determined by extravasated FITC-dextran (Fig. 5e–f), and this was prevented in platelet-depleted mice (Fig. 5g). To determine the role of E-selectin-induced αMβ2 activation, other groups of mice were treated with antibodies against E-selectin (9A9) or αMβ2 (M1/70) prior to the anti-H2d challenge. Vascular permeability was markedly reduced when either E-selectin or αMβ2 were inhibited (Fig. 5f). Furthermore, blocking E-selectin or αMβ2, but not P-selectin, strongly reduced lung injury (Fig. 5h). A similar protective effect was found when inhibitors of Src kinases, but not Syk or MAPK, were injected to mice prior to anti-MHC-I treatment (Supplementary Fig. 5). To investigate the potential role of tissue-damaging reactive oxygen species (ROS), we used a fluorescent probe to evaluate ROS formation by adherent neutrophils using MFIM. Anti-H2d infusion rapidly increased the frequency of ROS-producing adherent leukocytes (Fig. 5i and Supplementary Fig. 6). Platelet depletion or E-selectin inhibition prior to anti-H2d treatment markedly reduced the number of ROS-producing leukocytes (Fig. 5i). In agreement with these observations, pretreatment with n-acetyl-cysteine, a ROS-scavenging molecule, completely prevented the vascular permeability (Supplementary Fig. 7) and lung injury induced by anti-H2d (Fig. 5j). Taken together, the data suggest that E-selectin-induced αMβ2 activation mediates platelet capture at the leading edge of neutrophils, and that αMβ2 engagement, in turn, triggers the generation of ROS that produce vascular and organ injury.

Sickle RBC-neutrophil interactions trigger vaso-occlusion in SCD

The interactions between sRBCs and adherent leukocytes can trigger VOC and death in a humanized model of SCD21. In SCD mice, the surgical trauma induced a robust recruitment of leukocytes in venules in the first 90 min after surgery (Supplementary Fig. 8). Recordings of the same venules after systemic administration of TNF-α, 91–180 and 181–270 min after surgery, revealed further increase in leukocyte recruitment (Supplementary Fig. 8). A fraction of circulating sRBCs were captured by adherent leukocytes and the rate of interactions per leukocyte increased by the administration of TNF-α (Fig. 6a and Supplementary Fig. 8), eventually leading to reductions in blood flow, often leading to the animal's death21. Notably, the rate of RBC-leukocyte interactions was significantly elevated in SCD mice compared to control animals (1.88 ± 0.66 vs. 0.26 ± 0.04 interactions per leukocyte per min at >90 min after TNF-α injection, $p<0.001$). Using high-speed MFIM, we previously identified PMNs as the leukocyte subset mediating the vast majority of sRBC captures in SCD25. The induction of sRBC-leukocyte interactions after cytokine administration was not due to the recruitment of more neutrophils at later times because the proportion of adherent $CD45^+$ $Gr\text{-}1^+$ $F4/80^-$ PMNs, relative to adherent lymphocytes and monocytes, did not significantly change during the three viewing periods (Supplementary Fig. 9).

To determine whether E-selectin was involved in the increased frequency of heterotypic interactions observed in sickle mice after TNF-α administration, we generated SCD mice lacking endothelial E-selectin or P-selectin by transplanting bone marrow from SCD mice into lethally irradiated *Sele*$^{-/-}$ or *Selp*$^{-/-}$ mice, or blocked these adhesion molecules in SCD mice using monoclonal antibodies. While the number of adherent leukocytes recruited in the three viewing periods were similar to control SCD mice (Supplementary Fig. 10), the number of sRBC interactions per leukocyte was dramatically reduced in the absence of functional E-selectin (Fig. 6a), resulting in significant improvement in blood flow in the microcirculation (Fig. 6b). Moreover, the absence of functional E-selectin improved the survival of SCD mice during the experimental period (Supplementary Table 1). In contrast, absence or inhibition of P-selectin had a partial effect, with the number of interactions, flow rates and survival similar to those of SCD control mice at the later time points (Fig. 6a–b and Supplementary Table 1).

Elevated αMβ2 activity on SCD adherent leukocytes mediates VOC

The increased rate of sRBC captures in SCD mice compared to nRBC interactions in wild-type mice suggested that αMβ2 activity was upregulated on adherent PMNs in SCD mice. *In vivo* analysis of αMβ2 activity on SCD adherent leukocytes revealed a marked increase in the number of captured fluospheres compared to control hemizygous animals (3-fold increase, $p<0.0001$; Fig. 6c–d). This was largely due to the presence of a subset of leukocytes exhibiting marked integrin activation since 18% of adherent leukocytes in SCD mice captured ≥ 8 beads compared to 1.5% in hemizygous animals (Supplementary Fig. 11). Moreover, in the absence of E-selectin, αMβ2 activity on adherent leukocytes was reduced in SCD mice to levels similar to those found in control hemizygous animals (Fig. 6d). These results further emphasize the critical role of E-selectin in regulating regional αMβ2 activity on adherent PMNs.

To test whether αMβ2 mediates sRBC-leukocyte interactions, SCD mice were injected with anti-αMβ2 or isotype control antibody 70 min after injection of TNF-α (Fig. 6e). Anti-αMβ2 administration reduced the interactions between sRBCs and leukocytes by 79%, compared with control antibody (Fig. 6f). Further, anti-αMβ2 treatment significantly increased the wall shear rates (740 ± 62 s^{-1} in isotype control vs 933 ± 58 s^{-1} in M1/70-treated mice; $p<0.05$) and significantly prolonged survival after TNF-α treatment (Fig. 6g). These data indicate that E-selectin expressed during the inflammatory response triggers regional activation of leukocyte αMβ2 that promotes sRBC interactions with intravascular leukocytes and VOC in SCD mice.

DISCUSSION

Intravascular accumulation and activation of PMNs to localized inflamed areas can result in vascular and organ damage. Beyond its role in promoting the recruitment of inflammatory leukocytes, we show here that the endothelium sends activating signals that are critical for vascular injury. We have found that these E-selectin-mediated signals are transduced via ESL-1 and locally activate the integrin αMβ2 at the leading edge of crawling neutrophils. Luminal, activated αMβ2 clusters mediate heterotypic interactions with circulating RBCs

and platelets, which can produce vascular occlusion or damage. The protection from organ injury or death by targeting this pathway in two distinct disease models suggests that this paradigm may have broad implications in other thrombo-inflammatory diseases.

A primary source of leukocyte activating signals derive from GPCRs which upregulate integrin binding activity and promote arrest of rolling leukocytes29,30. Much less is known, however, about the events taking place after leukocytes have adhered. MFIM analyses have revealed that most adherent myeloid leukocytes (Gr-1$^+$) are actively migrating, presumably searching for a site of extravasation25, and exhibit a polarized appearance *in vivo* with clustered L-selectin at the uropod25. We used this marker to map the heterotypic interactions at the leading edge of crawling PMNs during inflammatory conditions, and show that although αMβ2 integrin was expressed homogenously on the cell surface, its activity was specifically enhanced at the leading edge. Leukocyte polarity is critical for their migration as cells must reorganize chemokine receptors, integrins, and various signaling and cytoskeletal constituents for directional migration14. Here, we have uncovered that clustered activation of a leukocyte integrin was directly involved in disease pathogenesis through the generation of intravascular heterotypic interactions.

In vitro studies have shown that endothelial selectins can transduce signals into leukocytes7,28,33,34. *In vivo*, PSGL-1 signaling through Syk can activate αLβ2 favoring slow rolling on ICAM-15, whereas CD44 can induce receptor clustering on slow rolling leukocytes through p38 signalilng4. The present studies suggest that a third physiological selectin ligand, ESL-1, is clearly a functional signaling receptor but that these signals are transmitted, unexpectedly, much later during the inflammatory cascade. These signals are transduced at least in part by Src kinases and affect the behavior of leukocytes that have adhered firmly, resulting in regional activation of αMβ2. Although the Src inhibitor used in these experiments (PP2) could potentially affect the activity of other kinases, the lower IC_{50} values for Src family members and the similar contribution to modulating αMβ2 activity found in animals with genetic deficiency in these kinases16, support a role for Src kinases in this ESL-1-mediated signaling. These observations highlight the signaling diversity of ESLs that produces distinct activating phenomena in neutrophils. While P-selectin can also activate αMβ2 through Src kinases at early stages of leukocyte recruitment to favor adhesion35, we show that this selectin is not required for the induction of heterotypic interactions in arrested leukocytes. Thus, the timing of αMβ2 activation may dictate the neutrophil response in inflamed venules.

The present study also underscores the bidirectional signaling capacity of αMβ2 integrin; ESL-1 can trigger “inside-out” αMβ2 activation at the leading edge of PMNs, while in turn the engagement of platelets by activated αMβ2 can trigger “outside-in” signals generating ROS36,37 that produce vascular damage in a model of TRALI. Engagement of αMβ2 has been shown to induce granular release and elicit vascular damage in a model of hemorrhagic vasculitis16. Interactions of platelets with neutrophils through P-selectin and PSGL-1 may also contribute to lung injury after acid challenge38, raising the intriguing possibility that different stimuli may promote inflammation through distinct leukocyte microdomains. Since the infusion of the anti-H2d antibody causes vascular injury outside the lung17, we have used high-speed MFIM in the cremasteric microcirculation as a platform to obtain

mechanistic insight. Our results suggest that E-selectin is necessary to initiate a second wave of activation that upregulates αMβ2 at the leading edge of neutrophils, allowing platelet capture which induces the formation of ROS by neutrophils and leads to vascular damage.

Significant mechanistic differences in leukocyte recruitment have been noted for the lung compared to other tissues39. For example, neutrophils do not require selectin-mediated rolling to sequester in the lung. However, the E-selectin-mediated secondary wave of activation described herein occurs after the canonical rolling step, when neutrophils are crawling in inflamed venules. Several studies have documented the induction of E-selectin expression in the lung microvasculature after inflammatory stimuli. Although we cannot be certain that our MFIM observations in the cremasteric venules reflect the events in the pulmonary microcirculation, we show that all the key functional players affecting permeability in the cremasteric vasculature during TRALI (E-selectin, αMβ2, platelets and ROS) are also critical for lung injury, suggesting that the same fundamental mechanisms are at work in both tissues.

We have identified complement C3 as one of the physiological αMβ2 ligands involved in RBC interactions, possibly through coating of aged or damaged RBCs40. Elevated levels of C3-bound to deoxygenated sRBC or RBC from hospitalized SCD patients have been observed41, suggesting that C3 may indeed play an important role in the pathogenesis of VOC. Another candidate ligand for αMβ2 expressed on sRBC that could be involved in these interactions is LW/ICAM-442, whose contribution to VOC alone or in conjunction with C3 deserves future attention. The physiological function of the inducible interactions between normal RBCs and adherent PMNs during inflammation remains undetermined. It may serve a hemostatic role by removing damaged or old RBCs, or by modulating platelet function through the release of adenosine diphosphate43 or other ADP-independent44 pathways by proximal RBCs. Numerous clinical studies have linked leukocytosis with ischemic heart disease45. Alterations of vascular permeability induced by leukocyte recruitment might be associated with a greater need for platelet adhesion to maintain vascular integrity during an inflammatory challenge. Notably, RBC interactions were most prevalent at relatively low shear rates, which is consistent with *in vitro* studies using microcapillary flow chambers46. PMN activation may cause vessel wall injury that could eventually lead to deep vein thrombosis47.

Because G-CSF administration can enhance E-selectin ligand expression on human leukocytes48, our data provide a mechanistic explanation for the severe complications observed in G-CSF-treated SCD patients, including the induction of sickle cell crises and acute lung injury15,49, and the predisposition for TRALI in patients treated with this cytokine23. Further, these observations offer novel candidate targets for the rational design of therapies for SCD, TRALI and possibly of other inflammatory or ischemic vascular diseases.

METHODS

Mice

C57BL/6 and Balb/c mice were purchased from National Cancer Institute. Berkeley sickle cell mice [Tg(Hu-miniLCR$\alpha 1^{G}\gamma^{A}\gamma\delta\beta^{S}$) Hb$\alpha^{-/-}$ Hb$\beta^{-/-}$], referred to as SCD mice, and control hemizygous mice [Tg(Hu-miniLCR$\alpha 1^{G}\gamma^{A}\gamma\delta\beta^{S}$) Hb$\alpha^{-/-}$ Hb$\beta^{+/-}$] mice have been previously described21,50. Both SCD mice are from a mixed background (H2b haplotype with contributions from C57BL/6, 129Sv, FVB/N, DBA/2, Black Swiss)21. *Cd44*$^{-/-}$, *Itgam*$^{-/-}$ and *C3*$^{-/-}$ animals were purchased from the Jackson Laboratory. The *Selplg*$^{-/-}$, *Selp*$^{-/-}$ and *Sele*$^{-/-}$ were backcrossed into the C57BL/6 background for at least 7 generations. Genotypes of all mice were determined by PCR. All animals were housed at the Mount Sinai School of Medicine barrier facility. Experimental procedures performed on the animals were approved by the Animal Care and Use Committee of Mount Sinai.

Bone marrow transplantation

SCD mice with or without additional genetic deficiencies were generated by transplantation of bone marrow nucleated cells into lethally irradiated recipients as described20.

Brightfield intravital microscopy

Brightfield intravital microscopy was performed as previously reported20,21. For SCD mice, several postcapillary and collecting venules were recorded from 15 min after the surgical preparation (time=0 is surgical section of the cremaster) for 75 minutes (pre-TNF-α), with each venule recorded continuously for at least 2 min. SCD mice were then injected i.p. with 0.5 μg recombinant murine TNF-α (R & D Systems) and then the same venules were videotaped over a period of 90 min (91–180 min), after which venules were recorded again for another 90 min (181–270 min). The role of endothelial selectins was evaluated in identical experiments performed in *Selp*$^{-/-}$ or *Sele*$^{-/-}$ mice transplanted with bone marrow cells from SCD donor mice, or using antibodies against P- or E- selectin (1 mg/kg) prior to surgery. In some experiments, 1 mg/kg of antibody against αM integrin (clone M1/70) subunit or IgG isotype control (IgG2b,κ) were infused through a carotid artery catheter into animals 70 min after treatment with TNF-α. In experiments with non-SCD C57BL/6 mice, TNF-α was administered intrascrotally and images recorded 160–210 min after cytokine injection. In some experiments, mice were injected with Src inhibitor PP2 (150 μg/kg), of SB203580 (100 μg; both from Calbiochem), or piceatannol (1 mg; Alexis Biochemicals), or an equivalent volume of vehicle (dimethyl sulfoxide) 120 min after TNF-α administration.

Hemodynamic measurements and image analyses for brightfield intravital microscopy

The venular diameter was measured using a video caliper. Centerline RBC velocity was measured for each venule in real time using an optical Doppler velocimeter (Texas A&M). Wall shear rate (γ) was calculated based on Poiseuille's law for a Newtonian fluid, $\gamma = 2.12 (8V_{mean}) / D_v$, where D_v is the venule diameter, V_{mean} is estimated as $V_{RBC} / 1.6$, and 2.12 is a median empirical correction factor obtained from actual velocity profiles measured in microvessels *in vivo*. Blood flow rate was calculated from the formula: $V_{mean} \times \pi \times d2/4$. All analyses were made using playback assessment of videotapes as previously described20,21.

High-speed multichannel fluorescence intravital microscopy

Mice were prepared for intravital microscopy as indicated above. All movies were acquired with an Olympus BX61WI workstation using LumPlanFl 60x objective NA 0.90 W or 10x objective NA 0.30 W, as previously described25 and analyzed using the SlideBook® software (Intelligent Imaging Innovations). Detailed description of the *in vivo* identification of adherent leukocytes on inflamed venules, identification and quantitation of platelet interactions, analysis of ESL-1 function, identification of leukocyte microdomains involved in RBC and platelet interactions, and analysis of vascular permeability are provided in the Supplementary Material.

Analysis of hemodynamic parameters in MFIM experiments

Centerline RBC velocities (V_{RBC}), wall shear rates (γ) and blood flow rates were calculated as indicated above. For experiments in which fluospheres were injected, V_{RBC} values were calculated by dividing the distance traveled by the fastest free flowing bead per frame by 0.022 s (capture rate: 45 frames per second = 22 ms / frame).

Statistical analyses

Unless otherwise indicated, data are presented as mean ± SEM and analyzed as follows: parametric data (lung injury, microdomain analysis and hemodynamic analyses) were analyzed using the ANOVA t-test for two groups or with Tukey's multigroup comparison or Bonferroni's correction for more than two groups. Statistical significance for non-parametric distributions (RBC-, platelet- or fluosphere-leukocyte interactions, vascular permeability and ROS production) was assessed using the Mann-Whitney test for two groups or the Kruskal-Wallis test with Dunn's multigroup comparison for more than two groups. A *p* value below 0.05 was deemed significant. GraphPad Prism or Excel softwares were used for analyses.

Supplementary Material

Refer to Web version on PubMed Central for supplementary material.

ACKNOWLEDGEMENTS

We thank Dr. C. Jakubzick (Mount Sinai School of Medicine) for help establishing the lung injury model and Dr. B. Wolitzky (Immune Tolerance Network; Bethesda, MD) for the anti-E-selectin 9A9 antibody. This work was supported by US National Institutes of Health grants R01 HL69438 to P.S.F. and T32 HL07824 to JC, and a Scientist Development Grant from the American Heart Association to A.H. (0735165N). P.S.F. is supported by an Established Investigator Award from the American Heart Association.

REFERENCES

1. Bullard DC, et al. Infectious susceptibility and severe deficiency of leukocyte rolling and recruitment in E-selectin and P-selectin double mutant mice. J Exp Med. 1996; 183:2329–2336. [PubMed: 8642341]
2. Frenette PS, Mayadas TN, H R, Hynes RO, Wagner DD. Susceptibility to infection and altered hematopoiesis in mice deficient in both P-and E-selectins. Cell. 1996; 84:563–574. [PubMed: 8598043]
3. Labow MA, et al. Characterization of E-selectin-deficient mice: Demonstration of overlapping function of the endothelial selectins. Immunity. 1994; 1:709–720. [PubMed: 7541306]

4. Hidalgo A, Peired AJ, Wild MK, Vestweber D, Frenette PS. Complete identification of E-selectin ligands on neutrophils reveals distinct functions of PSGL-1, ESL-1, and CD44. Immunity. 2007; 26:477–489. [PubMed: 17442598]
5. Zarbock A, Lowell CA, Ley K. Spleen tyrosine kinase Syk is necessary for E-selectin-induced alpha(L)beta(2) integrin-mediated rolling on intercellular adhesion molecule-1. Immunity. 2007; 26:773–783. [PubMed: 17543554]
6. Steegmaier M, et al. The E-selectin-ligand ESL-1 is a variant of a receptor for fibroblast growth factor. Nature. 1995; 373:615–620. [PubMed: 7531823]
7. Lo SK, et al. Endothelial-leukocyte adhesion molecule 1 stimulates the adhesive activity of leukocyte integrin CR3 (CD11b/CD18, Mac-1, alpha m beta 2) on human neutrophils. J Exp Med. 1991; 173:1493–1500. [PubMed: 1709677]
8. Simon SI, Hu Y, Vestweber D, Smith CW. Neutrophil tethering on E-selectin activates beta 2 integrin binding to ICAM-1 through a mitogen-activated protein kinase signal transduction pathway. J Immunol. 2000; 164:4348–4358. [PubMed: 10754335]
9. Gahmberg CG, Tolvanen M, Kotovuori P. Leukocyte adhesion--structure and function of human leukocyte beta2-integrins and their cellular ligands. Eur J Biochem. 1997; 245:215–232. [PubMed: 9151947]
10. Beller DI, Springer TA, Schreiber RD. Anti-Mac-1 selectively inhibits the mouse and human type three complement receptor. J Exp Med. 1982; 156:1000–1009. [PubMed: 7153706]
11. Simon DI, et al. Platelet glycoprotein ibalpha is a counterreceptor for the leukocyte integrin Mac-1 (CD11b/CD18). J Exp Med. 2000; 192:193–204. [PubMed: 10899906]
12. Barreiro O, de la Fuente H, Mittelbrunn M, Sanchez-Madrid F. Functional insights on the polarized redistribution of leukocyte integrins and their ligands during leukocyte migration and immune interactions. Immunol Rev. 2007; 218:147–164. [PubMed: 17624951]
13. Tohyama Y, et al. The critical cytoplasmic regions of the alphaL/beta2 integrin in Rap1-induced adhesion and migration. Mol Biol Cell. 2003; 14:2570–2582. [PubMed: 12808052]
14. Ridley AJ, et al. Cell migration: integrating signals from front to back. Science. 2003; 302:1704–1709. [PubMed: 14657486]
15. Abboud M, Laver J, Blau CA. Granulocytosis causing sickle-cell crisis. Lancet. 1998; 351:959. [PubMed: 9734950]
16. Hirahashi J, et al. Mac-1 signaling via Src-family and Syk kinases results in elastase-dependent thrombohemorrhagic vasculopathy. Immunity. 2006; 25:271–283. [PubMed: 16872848]
17. Looney MR, Su X, Van Ziffle JA, Lowell CA, Matthay MA. Neutrophils and their Fc gamma receptors are essential in a mouse model of transfusion-related acute lung injury. J Clin Invest. 2006; 116:1615–1623. [PubMed: 16710475]
18. Frenette PS, Atweh GF. Sickle cell disease: old discoveries, new concepts, and future promise. J Clin Invest. 2007; 117:850–858. [PubMed: 17404610]
19. Stuart MJ, Nagel RL. Sickle-cell disease. Lancet. 2004; 364:1343–1360. [PubMed: 15474138]
20. Chang J, Shi PA, Chiang EY, Frenette PS. Intravenous immunoglobulins reverse acute vaso-occlusive crises in sickle cell mice through rapid inhibition of neutrophil adhesion. Blood. 2008; 111:915–923. [PubMed: 17932253]
21. Turhan A, Weiss LA, Mohandas N, Coller BS, Frenette PS. Primary role for adherent leukocytes in sickle cell vascular occlusion: a new paradigm. Proc Natl Acad Sci U S A. 2002; 99:3047–3051. [PubMed: 11880644]
22. Holness L, Knippen MA, Simmons L, Lachenbruch PA. Fatalities caused by TRALI. Transfus Med Rev. 2004; 18:184–188. [PubMed: 15248168]
23. Silliman CC, Ambruso DR, Boshkov LK. Transfusion-related acute lung injury. Blood. 2005; 105:2266–2273. [PubMed: 15572582]
24. Falati S, Gross P, Merrill-Skoloff G, Furie BC, Furie B. Real-time in vivo imaging of platelets, tissue factor and fibrin during arterial thrombus formation in the mouse. Nat Med. 2002; 8:1175–1181. [PubMed: 12244306]
25. Chiang EY, Hidalgo A, Chang J, Frenette PS. Imaging receptor microdomains on leukocyte subsets in live mice. Nat Methods. 2007; 4:219–222. [PubMed: 17322889]

26. Totani L, et al. Src-family kinases mediate an outside-in signal necessary for beta2 integrins to achieve full activation and sustain firm adhesion of polymorphonuclear leucocytes tethered on E-selectin. Biochem J. 2006; 396:89–98. [PubMed: 16433632]
27. Smith ML, Olson TS, Ley K. CXCR2- and E-selectin-induced neutrophil arrest during inflammation in vivo. J Exp Med. 2004; 200:935–939. [PubMed: 15466624]
28. Simon SI, et al. L-selectin (CD62L) cross-linking signals neutrophil adhesive functions via the Mac-1 (CD11b/CD18) beta 2-integrin. J Immunol. 1995; 155:1502–1514. [PubMed: 7543524]
29. Butcher EC. Leukocyte-endothelial cell recognition: three (or more) steps to specificity and diversity. Cell. 1991; 67:1033–1036. [PubMed: 1760836]
30. Lawrence MB, Springer TA. Leukocytes roll on a selectin at physiologic flow rates: distinction from and prerequisite for adhesion through integrins. Cell. 1991; 65:859–873. [PubMed: 1710173]
31. Barreiro O, et al. Dynamic interaction of VCAM-1 and ICAM-1 with moesin and ezrin in a novel endothelial docking structure for adherent leukocytes. J Cell Biol. 2002; 157:1233–1245. [PubMed: 12082081]
32. Carman CV, Springer TA. A transmigratory cup in leukocyte diapedesis both through individual vascular endothelial cells and between them. J Cell Biol. 2004; 167:377–388. [PubMed: 15504916]
33. Lorant DE, et al. Inflammatory roles of P-selectin. J Clin Invest. 1993; 92:559–570. [PubMed: 7688760]
34. Evangelista V, et al. Platelet/polymorphonuclear leukocyte interaction: P-selectin triggers protein-tyrosine phosphorylation-dependent CD11b/CD18 adhesion: role of PSGL-1 as a signaling molecule. Blood. 1999; 93:876–885. [PubMed: 9920836]
35. Wang HB, et al. P-selectin primes leukocyte integrin activation during inflammation. Nat Immunol. 2007; 8:882–892. [PubMed: 17632516]
36. Shappell SB, et al. Mac-1 (CD11b/CD18) mediates adherence-dependent hydrogen peroxide production by human and canine neutrophils. J Immunol. 1990; 144:2702–2711. [PubMed: 2181020]
37. Husemann J, Obstfeld A, Febbraio M, Kodama T, Silverstein SC. CD11b/CD18 mediates production of reactive oxygen species by mouse and human macrophages adherent to matrixes containing oxidized LDL. Arterioscler Thromb Vasc Biol. 2001; 21:1301–1305. [PubMed: 11498457]
38. Zarbock A, Singbartl K, Ley K. Complete reversal of acid-induced acute lung injury by blocking of platelet-neutrophil aggregation. J Clin Invest. 2006; 116:3211–3219. [PubMed: 17143330]
39. Doerschuk CM. Mechanisms of leukocyte sequestration in inflamed lungs. Microcirculation. 2001; 8:71–88. [PubMed: 11379793]
40. Lutz HU, et al. Naturally occurring anti-band-3 antibodies and complement together mediate phagocytosis of oxidatively stressed human erythrocytes. Proc Natl Acad Sci U S A. 1987; 84:7368–7372. [PubMed: 3313392]
41. Wang RH, Phillips G Jr, Medof ME, Mold C. Activation of the alternative complement pathway by exposure of phosphatidylethanolamine and phosphatidylserine on erythrocytes from sickle cell disease patients. J Clin Invest. 1993; 92:1326–1335. [PubMed: 7690777]
42. Zennadi R, et al. Role and regulation of sickle red cell interactions with other cells: ICAM-4 and other adhesion receptors. Transfus Clin Biol. 2008; 15:23–28. [PubMed: 18502676]
43. Gaarder A, Jonsen J, Laland S, Hellem A, Owren PA. Adenosine diphosphate in red cells as a factor in the adhesiveness of human blood platelets. Nature. 1961; 192:531–532. [PubMed: 13896038]
44. Santos MT, et al. Enhancement of platelet reactivity and modulation of eicosanoid production by intact erythrocytes. A new approach to platelet activation and recruitment. J Clin Invest. 1991; 87:571–580. [PubMed: 1991840]
45. Coller BS. Leukocytosis and ischemic vascular disease morbidity and mortality: is it time to intervene? Arterioscler Thromb Vasc Biol. 2005; 25:658–670. [PubMed: 15662026]
46. Goel MS, Diamond SL. Adhesion of normal erythrocytes at depressed venous shear rates to activated neutrophils, activated platelets, and fibrin polymerized from plasma. Blood. 2002; 100:3797–3803. [PubMed: 12393714]

47. Wakefield TW, Myers DD, Henke PK. Mechanisms of venous thrombosis and resolution. Arterioscler Thromb Vasc Biol. 2008; 28:387–391. [PubMed: 18296594]

48. Dagia NM, et al. G-CSF induces E-selectin ligand expression on human myeloid cells. Nat Med. 2006; 12:1185–1190. [PubMed: 16980970]

49. Arimura K, et al. Acute lung Injury in a healthy donor during mobilization of peripheral blood stem cells using granulocyte-colony stimulating factor alone. Haematologica. 2005; 90 ECR10.

50. Paszty C, et al. Transgenic knockout mice with exclusively human sickle hemoglobin and sickle cell disease. Science. 1997; 278:876–878. [PubMed: 9346488]

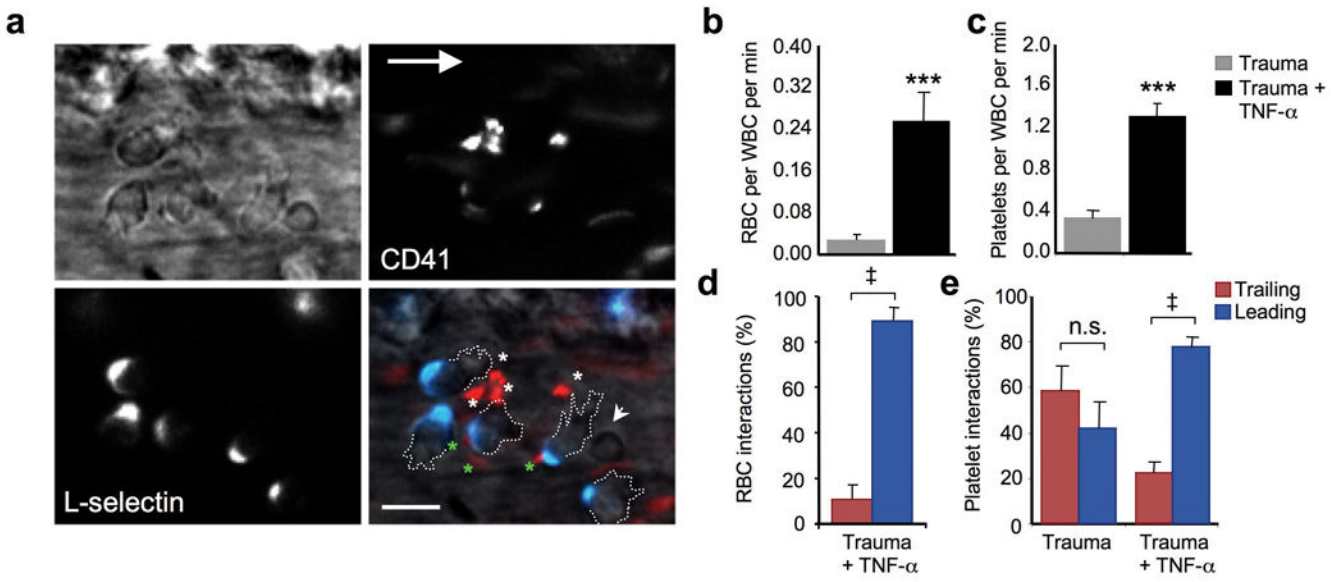

Figure 1. Heterotypic interactions of RBC and platelets with leukocyte microdomains are induced during inflammation

(a) Heterotypic interactions between leukocytes and platelets in a TNF-α- stimulated C57BL/6 mouse. Fluorescently conjugated antibodies to L-selectin (blue) and CD41 (red) allow identification of the trailing edge of crawling leukocytes and platelets, respectively. The short arrow indicates an interacting RBC, and the asterisks show interacting platelets (green for those mediated by the trailing edge, white for the leading edge). The large arrow points to the direction of blood flow. Scale bar = 10 μm. **(b)** Frequency of interactions between RBCs and leukocytes in venules of mice where surgical trauma or trauma plus TNF-α administration preceded imaging. n = 5 mice. ***, $p<0.001$, Mann-Whitney test. **(c)** Frequency of interactions between leukocytes and platelets. n=5–6 mice. ***, $p<0.001$, Mann-Whitney test. **(d)** Contribution of the leading and trailing edges in RBC interactions after TNF-α treatment. n = 4 mice; ‡, $p<0.005$. **(e)** Contribution of leukocyte microdomains to platelet interactions in wild-type mice, treated or not with TNF-α. n = 5 mice per group; ‡, $p<0.005$ compared to Trailing group, paired *t*-test; NS, not significant.

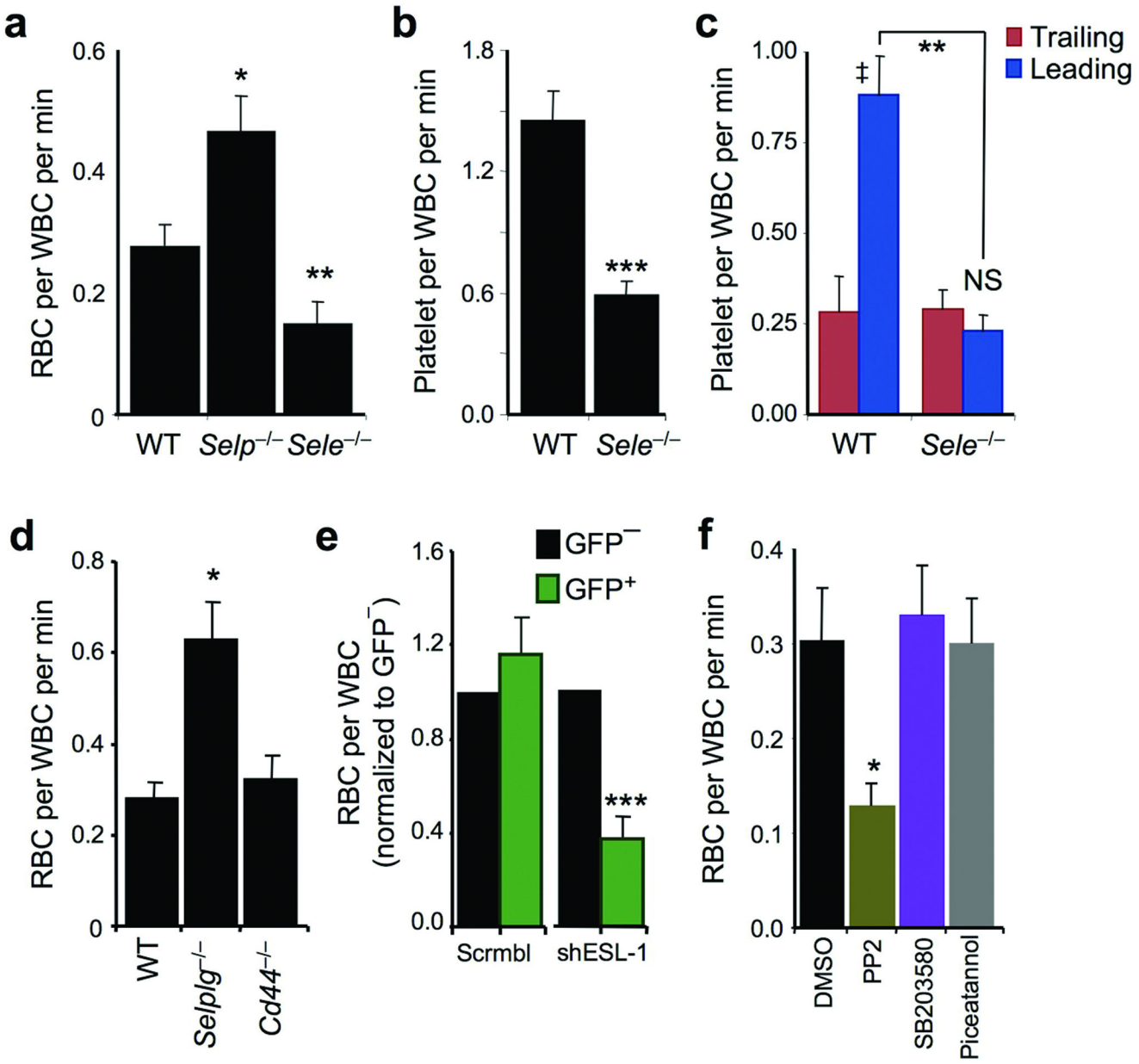

Figure 2. RBC and platelet interactions depend on E-selectin and its ligand ESL-1

(a) Number of RBC captures per adherent leukocyte in wild–type, *Selp*$^{-/-}$ and *Sele*$^{-/-}$ mice. n = 32–40 venules from 5–7 mice per group. *, p<0.05 compared to WT, **, p<0.01 compared to the other groups; Kruskal-Wallis test with Dunn's multigroup comparison. **(b)** Reduced number of platelet captures per adherent leukocyte in *Sele*$^{-/-}$ mice. n = 32–42 venules from at least 5 mice per group. ***, p<0.0001. **(c)** Contribution of leukocyte microdomains to platelet interactions in TNF-α-treated mice. n = 5 mice per group. **, p<0.01, Mann-Whitney test. ‡, p=0.003 and NS, not significant compared to Trailing groups, paired *t*-test. **(d)** RBC-leukocyte interactions in wild-type, *Selplg*$^{-/-}$ and *Cd44*$^{-/-}$ mice. n = 31–42 venules from 5–7 mice per group. *, p<0.05, Kruskal-Wallis test with

Dunn's multigroup comparison. **(e)** RBC captures by leukocytes transduced with control (Scrmbl) or shESL-1 lentiviral vectors. n = 4–6 mice per group. ***, $p<0.0001$ compared to GFP^- cells from the same lentiviral group, paired *t*-test. **(f)** nRBC interactions in mice pretreated with inhibitors to Src kinases (PP2), p38 MAPK (SB203580) or Syk (Piceatannol), or vehicle control (DMSO). n = 33–44 venules from 6 mice per group. *, $p<0.05$ compared to all other groups, Kruskal-Wallis test with Dunn's multigroup comparison.

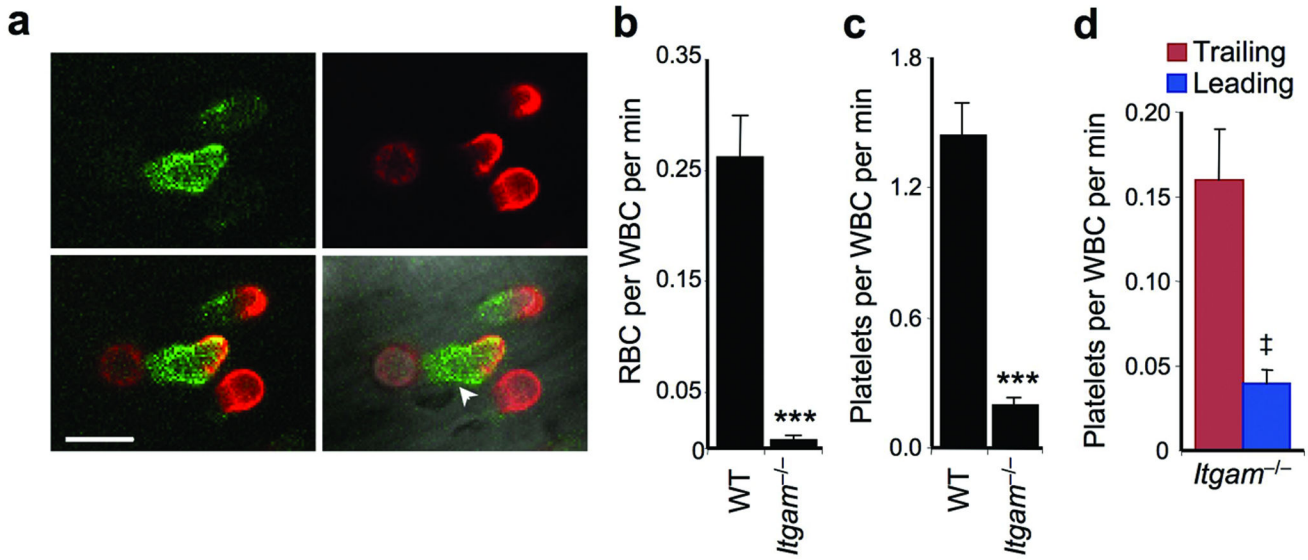

Figure 3. Heterotypic interactions with RBC and platelets are mediated by the leukocyte integrin αMβ2

(a) Micrographs of adherent leukocytes obtained by MFIM analyses of TNF-α-treated C57BL/6 mice injected with labeled antibodies against L-selectin (red) and anti-αM (green). αMβ2 integrin expression is homogenously distributed, including where an RBC (arrowhead) is shown interacting at the leading edge of an adherent leukocyte. Scale bar = 10 μm. **(b)** RBC-WBC interactions in *Itgam*$^{-/-}$ mice compared to wild-type (WT) controls. n = 41–42 venules from 6–7 mice per group. **, p<0.001, Mann-Whitney test. **(c)** Platelet–WBC interactions in *Itgam*$^{-/-}$ mice compared to WT. n = 35–36 venules from 5–6 mice per group. **, p<0.0001, Mann-Whitney test. **(d)** Contribution of leukocyte microdomains to platelet captures in TNF-α-treated *Itgam*$^{-/-}$ mice. n = 5 mice. ‡, p=0.008, paired *t*-test compared to Trailing values.

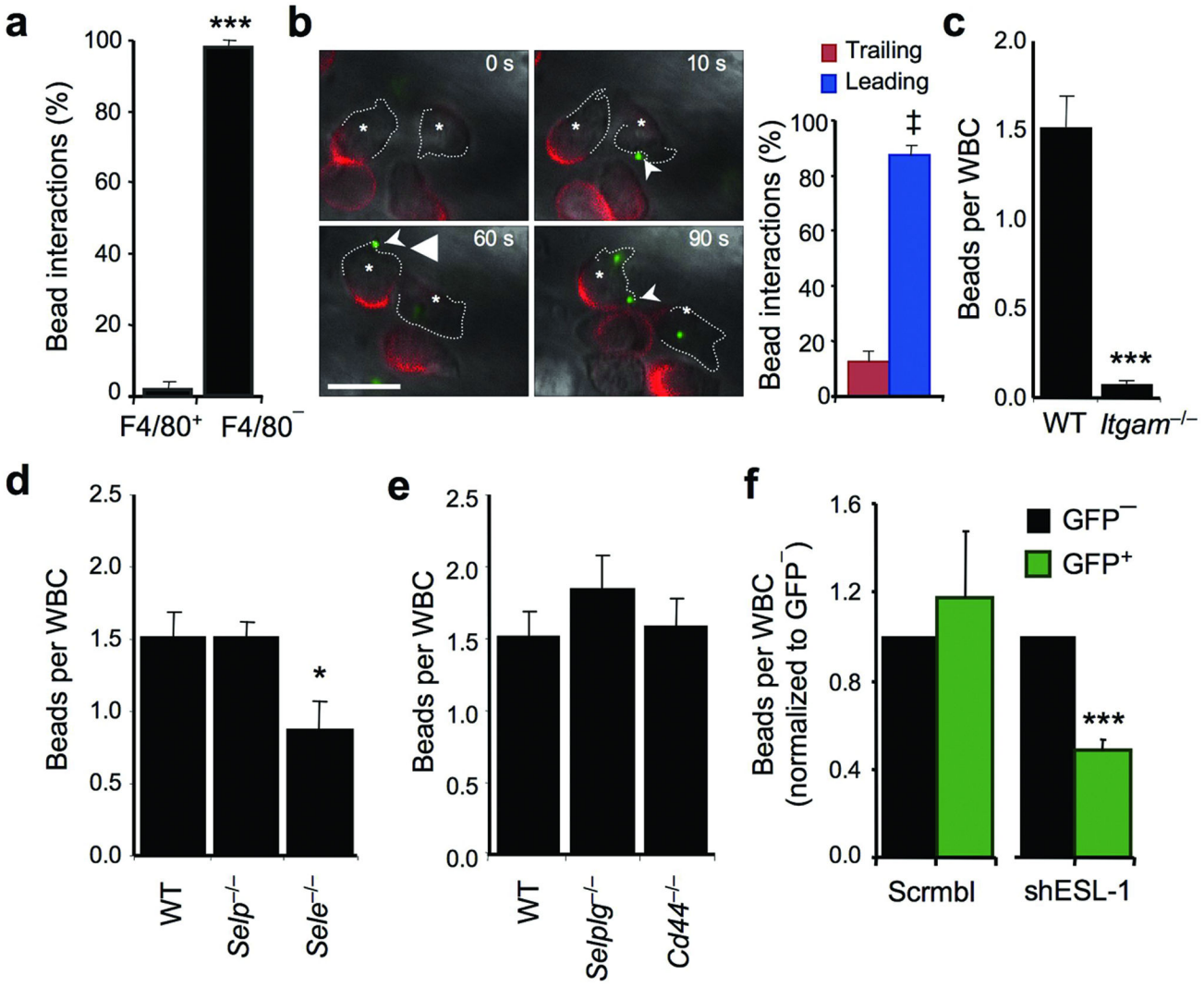

Figure 4. E-selectin and ESL-1 modulate regional αMβ2 activity on adherent leukocytes *in vivo*

(a) Frequency of fluosphere (beads) binding by F4/80^{-} and F4/80^{+} adherent leukocytes. Data obtained from analyses of 84 fluosphere captures from 4 mice. ***, p<0.001, *t*-test. **(b)** Time-lapse micrographs of *in vivo* fluosphere capture by two representative adherent leukocytes (asterisks). Leading edges are outlined with dotted lines and L-selectin clusters are in red. Sequence of capture of fluospheres at the times indicated. A movie depicting capturing events is shown in Supplementary Video 3. The histogram (right panel) shows the quantitation of the fluospheres captured by the leading and trailing edges from 98 events identified in 7 mice; ‡, p=0.0005. Scale bar = 10 μm. **(c)** Binding of albumin-coated fluospheres to leukocytes in wild-type and *Itgam*$^{-/-}$ mice. Each dot represents the average number of fluospheres bound per leukocyte in individual venules. n = 40 venules from 4–5 mice per group. **, p<0.001, Mann-Whitney test. **(d)** Binding of albumin-coated fluospheres to leukocytes in wild-type, *Selp*$^{-/-}$ and *Sele*$^{-/-}$ mice. n = 33–43 venules from 4–7 mice per group. *, p<0.05 compared to the other groups; Kruskal-Wallis test. **(e)** Binding of fluospheres in wild-type, *Selplg*$^{-/-}$ and *Cd44*$^{-/-}$ mice. n = 30–47 venules from 4–6 mice

per group. **(f)** Fluosphere capture in leukocytes transduced with shESL-1 or scrambled sequence lentiviral vectors. n = 5 mice per group. ***, $p<0.0001$ compared to GFP^- cells from the same lentiviral group, paired *t*-test.

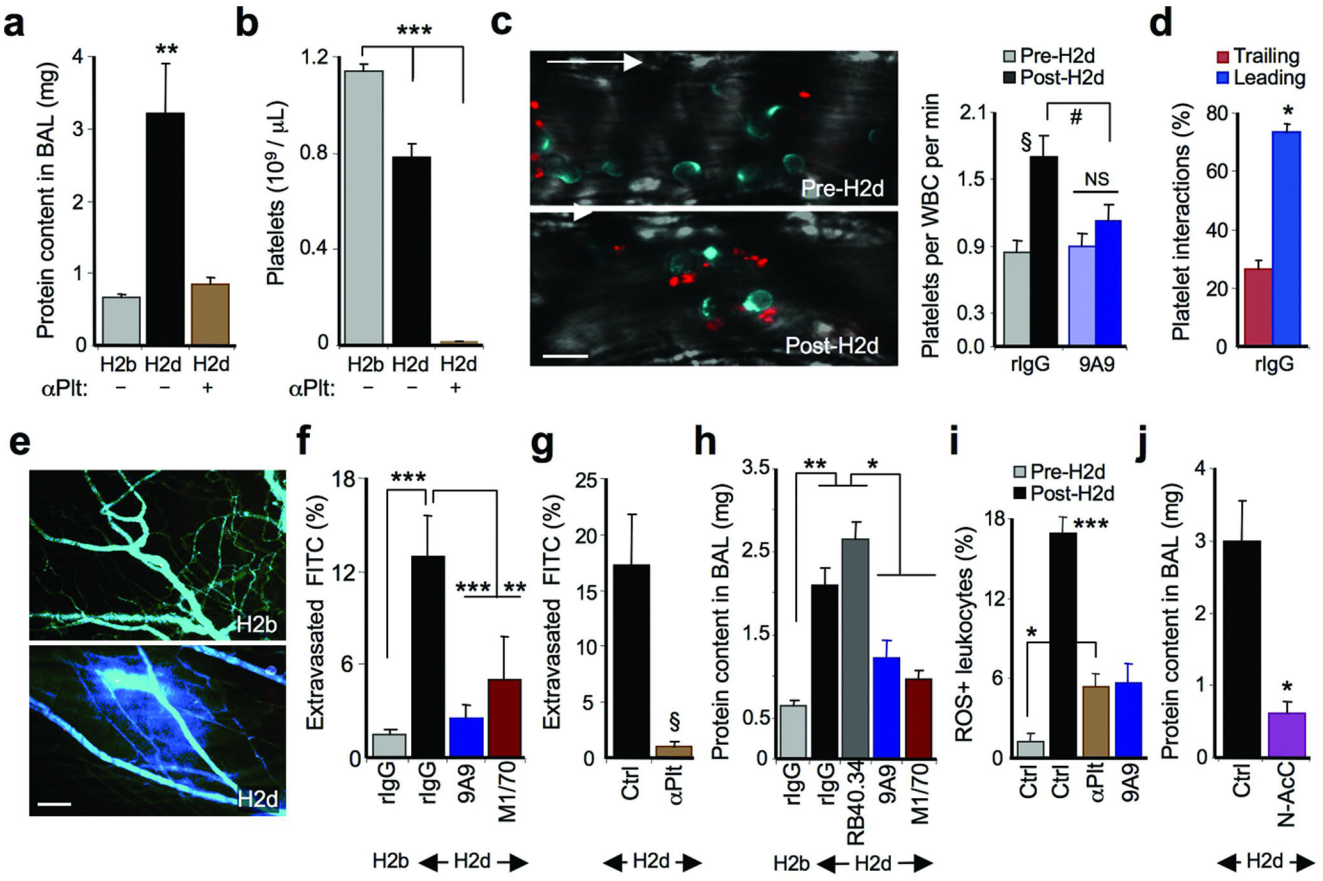

Figure 5. Antibody-induced lung injury requires platelet-leukocyte interactions and is blocked by antibodies to E-selectin and αMβ2

(a) Protein accumulation in BAL fluids after anti-H2b or H2d antibody administration. αPlt, platelet-depleted mice; n = 7–9 mice. **, p<0.01. **(b)** Platelet counts from mice in (a). n = 9–10 mice; ***, p<0.001. **(c)** Left panels are representative micrographs of platelet-leukocyte interactions before (pre-H2d) and after (post-H2d) anti-H2d administration (L-selectin, blue; CD41, red). Arrow, direction of flow. Scale bar = 10 μm. Right panel, frequency of platelet-leukocyte interactions in control or anti-E-selectin-treated (9A9) mice. §, p<0.01 and NS, not significant, paired t-test. #, p<0.05, unpaired *t*-test. **(d)** Contribution of microdomains to interactions in the rIgG group. n = 5 mice; *, p=0.01. **(e)** Representative micrographs depicting vascular permeability after anti-H2d or anti-H2b treatment (FITC-dextran, blue). Scale bar = 100 μm. **(f)** FITC-dextran extravasation in mice treated with rat IgG, anti-E-selectin (9A9) or anti-αMβ2 (M1/70) antibodies. n = 20–32 venules. **, p<0.01; ***, p<0.001. **(g)** FITC-dextran extravasation in platelet-depleted (αPlt) or control mice after anti-H2d administration. n = 16–20 venules. §, p = 0.002. **(h)** Effect of P-selectin (RB40.34), E-selectin (9A9) and αMβ2 (M1/70) inhibition in lung injury. n = 7–13 mice. *, p<0.05; **, p<0.001. **(i)** Percentage of ROS-positive adherent leukocytes in control (Ctrl), platelet-depleted (αPlt) or anti-E-selectin antibody-treated (9A9) mice; n = 30–53 venules. *, p<0.05; ***, p<0.001 compared to all other groups. **(j)** Protein content in BAL fluids of

mice treated with saline (Ctrl) or n-acetyl-cysteine (N-AcC). n = 5–14 mice. *, $p < 0.05$, unpaired *t*-test.

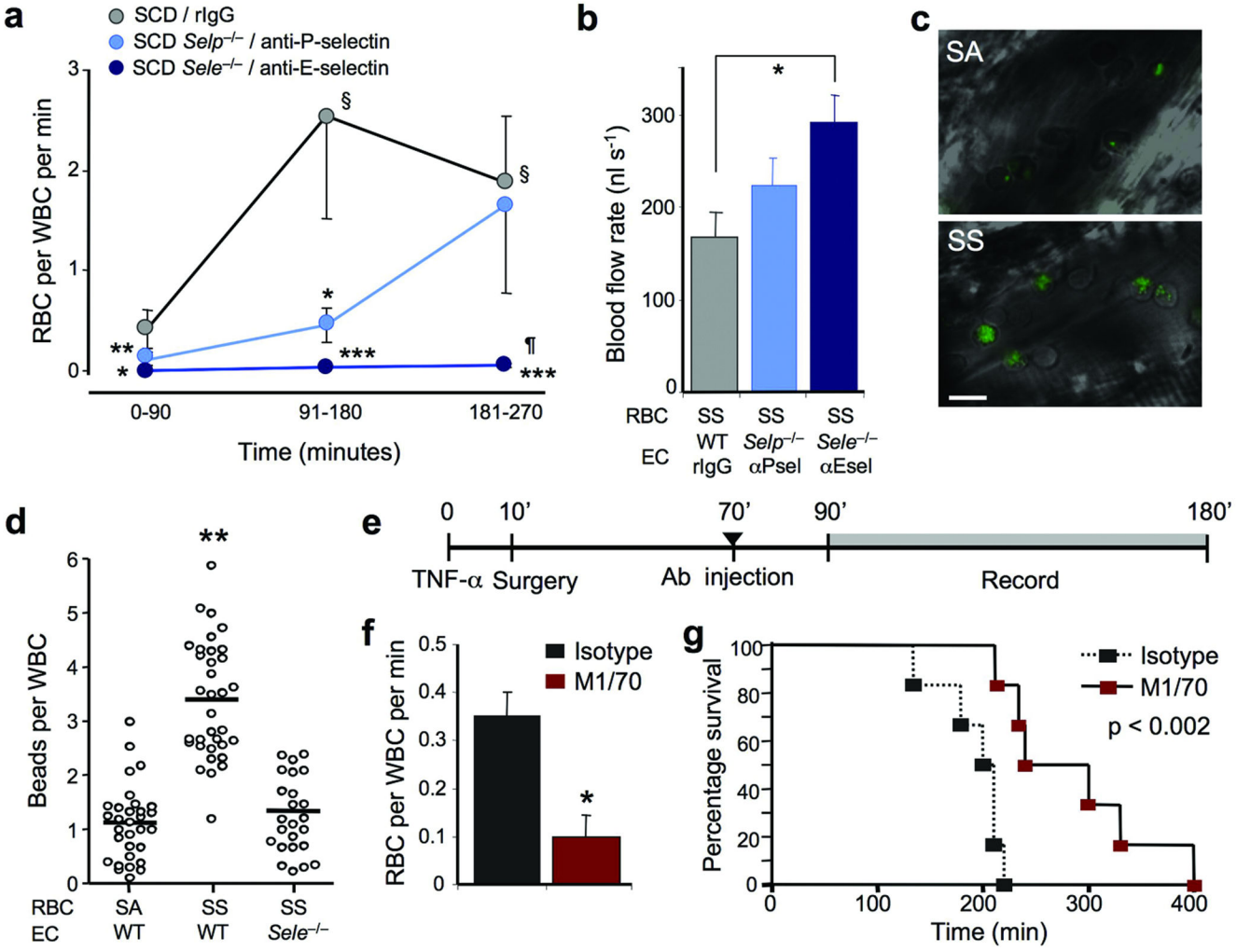

Figure 6. Vaso-occlusion in sickle cell disease requires E-selectin-mediated activation of αMβ2

(a) Individual contributions of P- and E-selectins in sRBC capture by adherent leukocytes using genetically deficient mice or function-blocking antibodies. n = 9–17 mice. §, p< 0.01 compared to time 0–90 in the same group; *, p<0.05; **, p<0.01; ***, p<0.01 compared to the SCD group at the same time point; ¶, p<0.05 compared to the SCD *Selp*$^{-/-}$ group at the same time point; Kruskal-Wallis test. **(b)** Analysis of blood flow rates from the experiments shown in (**a**), at the 181–270 time point. SS, sickle cell; n = 9–16 mice; *, p < 0.01, one-way ANOVA. **(c)** Representative micrographs showing albumin-coated fluospheres bound to adherent leukocytes in hemizygous (SA) or homozygous (SS) SCD mice. Scale bar = 10 μm. **(d)** Binding of albumin-coated fluospheres to leukocytes in SA and SS chimeras with wild-type endothelium or *Sele*$^{-/-}$ endothelium. Each circle represents the average number of fluospheres bound per leukocyte for an individual venule, and bars represent mean values. n = 24–34 venules from 3–5 mice per group. **, p<0.001 compared to the two other groups; Kruskal-Wallis test. **(e)** Experimental scheme to assess the role of αMβ2 in vaso-occlusion. **(f)** αMβ2 blockade reduced the number of sRBC interactions with leukocytes. n = 6 mice

per group; *, p = 0.001. **(g)** Kaplan-Meier survival curves after TNF-α treatment in control and M1/70 treated groups. n = 6 mice per group. Log-rank test, p< 0.002.